Available online at www.sciencedirect.com
SCIENCE DIRECT®
Journal of Pharmaceutical and Biomedical Analysis 38 (2005) 858–864
JOURNAL OF PHARMACEUTICAL AND BIOMEDICAL ANALYSIS
www.elsevier.com/locate/jpba

# Quantification of bambuterol hydrochloride in a formulated product using solid-state NMR

Robin K. Harris [a,*], Paul Hodgkinson [a], Tomas Larsson [b], Amsaveni Muruganantham [a]

[a] *Department of Chemistry, University of Durham, South Road, Durham DH1 3LE, UK*
[b] *AstraZeneca Research and Development, Analytical Development 5, Lund S-22187, Sweden*

Received 24 September 2004; received in revised form 15 January 2005; accepted 22 January 2005
Available online 24 May 2005

**Abstract**

Carbon-13 NMR spectra of the stable polymorphs of solid bambuterol hydrochloride (BHC) and terbutaline sulfate (TBS) are reported and the resonances assigned with the aid of solution-state spectra. A protocol is presented for quantification of BHC in a formulation in lactose, together with TBS, relative to a reference peak from magnesium stearate. This protocol compares the intensity of an aromatic signal of BHC with that of the main-chain methylene carbons of the stearate. It is shown that the limit of detection (LOD) of BHC in this system under the conditions described is 0.5% with an effective limit of quantification (LOQ) of 1.0%. A calibration plot for the quantification is presented and the various factors affecting the accuracy of the measurements are described. No discernible differences are found in the spectra of physical mixtures of the components, whole tablets, and crushed or ground tablets.
© 2005 Elsevier B.V. All rights reserved.

*Keywords:* Bambuterol hydrochloride; Terbutaline sulfate; Active pharmaceutical ingredient; CPMAS NMR; Quantification; Internal reference; Limit of detection; Limit of quantification; Error analysis

## 1. Introduction

Solid-state NMR has several advantages over other techniques [1–4] for the study of molecular-level structure and dynamics for compounds of pharmaceutical interest. It is non-destructive and highly versatile, since a variety of nuclides can be used and different pulse sequences employed to achieve different results. Moreover, information can be obtained for heterogeneous and amorphous materials as well as for homogeneous crystalline phases. Though solid-state NMR is in routine use for structure elucidation and characterization, only a few quantification studies have been reported in the literature [5–8]. There is, in particular, considerable interest in pharmaceutical industry in quantifying situations involving polymorphism in drug substances and for formulated products.

The pharmaceutical compounds examined in the present research are bambuterol hydrochloride, 5(2-(tert-butylamino)-1-hydroxyethyl)-*m*-phenylene-bis(dimethylcarbamate) hydrochloride (BHC, **I**) and terbutaline sulfate, 1-(3,3-dihydroxyphenyl)-2-*t*-butylaminoethanol sulfate (TBS, **II**). BHC is a pro-drug to the $\beta_2$-adrenoreceptor agonist terbutaline and both are used in asthma therapy. Three anhydrous polymorphs (I, II and III) have been identified so far [9], but no crystal structures for any of these forms of BHC have been reported in the Cambridge Structure Database (CSD). Three crystalline anhydrates (A, B and C′) of TBS have been identified so far [9]. Only the B form of TBS has had its crystal structure reported to date [10].

* Corresponding author. Tel.: +44 191 334 2021; fax: +44 191 384 4737.
*E-mail address:* r.k.harris@durham.ac.uk (R.K. Harris).

0731-7085/$ – see front matter © 2005 Elsevier B.V. All rights reserved.
doi:10.1016/j.jpba.2005.01.052

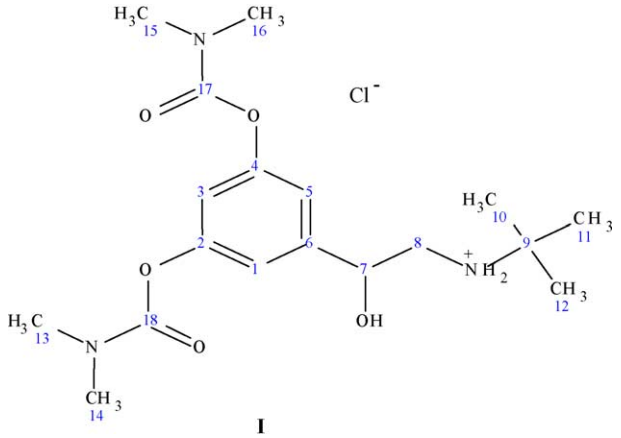


I

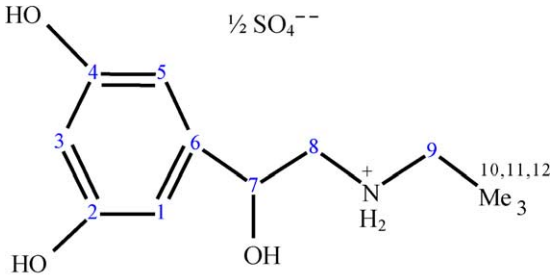


II

As part of our study, we report the $^{13}$C MAS NMR spectra of the polymorphs of BHC and TBS which are stable under ambient conditions, namely form I of BHC and form B of TBS. Samples including these forms of BHC and TBS formulated together in α-lactose monohydrate, as a filler, and magnesium stearate, as a lubricant, have also been studied with a view to obtaining a robust protocol for quantifying the amount of BHC and determining both the limit of detection (LOD) and the limit of quantification (LOQ) under conditions of acceptable spectrometer usage. Quantification has been done in four situations: (1) a physical mixture of the above components; (2) whole tablets; (3) mildly-crushed tablets and (4) finely-ground tablets.

Quantification may be carried out either by replacing the sample by a standard of known composition or by choosing a reference peak for a compound included in the sample in question. The latter procedure eliminates or minimises the effects of many spectrometer variables on the quantification measurement. For this reason, we have chosen to adopt a signal from one of the components of our simulated formulation, i.e. magnesium stearate.

There are various definitions of LOD and LOQ [11–13]. Among the possibilities listed for LOD [11], we choose to use a value based on a signal-to-noise ratio (S/N) of 3:1, with the noise level defined in terms of the root-mean-square standard deviation, though an alternative definition of LOD [14] refers to S/N of 2:1, with noise measured peak-to-peak. LOQ may be viewed as a S/N of 10 [11] or as the amount quantifiable with a variation coefficient not higher than 10% [12]. Our usage corresponds to the latter.

## 2. Experimental

### 2.1. Samples

The samples involved in this study have been provided by AstraZeneca R&D, Lund, Sweden. The physical mixtures of the formulated systems were prepared in the laboratory while the tablets were produced at AstraZeneca R&D, Charnwood, UK. To obtain homogeneous physical mixtures, the components were mixed well for ∼10 min using an electric mixer. The mildly and finely ground samples were prepared by crushing the tablets and grinding into fine powder, respectively. The composition of BHC was varied from 0 to 15% (w/w, %), by changing the BHC and relative α-lactose monohydrate composition while keeping the magnesium stearate (1%) and the TBS (5%) concentrations constant.

### 2.2. NMR

Solution-state spectra of BHC and TBS (in $D_2O$) were acquired on a Varian Inova 500 spectrometer (operating at 499.91 MHz for $^1$H and 125.70 MHz for $^{13}$C) to assist assignment of the solid-state spectra (see Tables 1 and 2). For all spectra a pulse angle of 45° was used with a recycle delay of 3 s for $^{13}$C but no delay for $^1$H. An HSQC experiment with

Table 1
Solution- and solid-state chemical shifts of BHC

| $^{13}$C atom | Solution-state chemical shift (ppm) | Solid-state chemical shift (ppm) |
|---|---|---|
| 1, 5, 3 | 116.3, 117.3 | 117.4, 118.8 |
| 2, 4 | 151.9 | 152.5, 153.6 |
| 6 | 143.1 | 146.8 |
| 7 | 68.7 | 69.7 |
| 8 | 47.6 | 47.7 |
| 9 | 57.7 | 58.2 |
| 10, 11, 12 | 24.9 | 23.3, 27.7 |
| 13, 14, 15, 16 | 36.4, 36.3 | 36.7, 38.3 |
| 17, 18 | 156.3 | 156.1, 158.4 |

Table 2
Solution- and solid-state chemical shifts of TBS

| $^{13}$C atom | Solution-state chemical shift (ppm) | Solid-state chemical shift (ppm) |
|---|---|---|
| 1, 5, 3 | 102.6, 105.0 | 104.2, 105.4, 106.4, 107.8, 108.6, 109.7 |
| 2, 4 | 157.1, 157.2 | 156.6, 157.9 |
| 6 | 143.0, 143.1 | 141.5, 143.4 |
| 7 | 69.0, 69.1 | 70.7, 72.0 |
| 8 | 47.5 | 47.1, 50.0 |
| 9 | 57.4 | 58.5 |
| 10, 11, 12 | 24.8 | 25.5 |

Fig. 1. View of the tablets and the rotor used.

gated decoupling and 1 s recycle delay was implemented on the Inova 500 to link the $^{1}$H and $^{13}$C resonances.

Carbon-13 CPMAS experiments were performed at 50 MHz on a Varian/Chemagnetics CMX200 spectrometer (unless otherwise mentioned) using a 7.5 mm probe with the following acquisition and processing parameters: spinning speed 5 kHz, number of acquisitions 2048, recycle delay 5 s and contact time 5 ms. All these parameters were optimised from experiments with pure BHC because it is the compound of interest. The rotor holds approximately 210 mg of sample or seven tablets (which had been specially prepared to match the inside diameter of the rotors, see Fig. 1). Selective spectra of the quaternary and methyl carbons were obtained using the dipolar dephasing ("non-quaternary suppression") pulse sequence [15].

## 3. Protocol for quantification

The following protocol has been devised for measurements of formulated systems, referring to the quantification of BHC in a formulated product for concrete examples. As with any protocol, it should be transferable to other spectrometers.

### *3.1. Spectrometer settings*

1. Choice of an appropriate probe is critical to obtaining satisfactory results in a reasonable period of time. Experiments on sensitive nuclei such as $^{1}$H and $^{19}$F, etc. can be performed using small (μl) sample quantities on probes taking small diameter rotors (e.g. 2.5 mm outside diameter). Quantification using $^{13}$C (receptivity of $\sim 10^{-4}$ relative to $^{1}$H) will require much larger sample volumes. On the 200 MHz system used here (relatively low magnetic field), 7.5 mm o.d. rotors were used (sample volume 450 μl). Intermediate sized rotors (e.g. 4–5 mm) may be more appropriate at higher fields. The acquisition times need to balance signal-to-noise (and hence accuracy) against the time for which a valuable resource is in use. Here we used total accumulation times of 3 h per sample.
2. The magic angle setting must be verified. This is conveniently done using the $^{79}$Br resonance of KBr, since the $^{13}$C and $^{79}$Br NMR frequencies are close. The setting is good if the rotational echo train extends to ∼10 ms. Depending on the probe design, the magic angle setting is generally stable over extended periods. It should, however, be checked whenever physical movement is possible, e.g. after variable-temperature experiments.
3. The probe must be correctly tuned for each sample studied, including the sample used to set up the cross-polarisation. The power reflected from the probe should be <5% of the input power on each rf channel. Poor or inconsistent tuning will reduce sensitivity and largely invalidate calibration experiments. If, however, tuning losses are consistently kept to negligible levels, minor variations in tuning will have no measurable impact on quantification.
4. Pulse durations and, if required, the Hartmann–Hahn condition for cross-polarisation need to be carefully calibrated to ensure maximum sensitivity. In this case, $^{1}\text{H} \rightarrow {}^{13}\text{C}$ cross-polarisation was set up using a sample of adamantane spinning relatively slowly (∼2 kHz). This is a convenient compound to use at lower magnetic fields because cross-polarisation set-up, checking field homogeneity and chemical shift referencing can be set using this single sample. Once the cross-polarisation condition has been set (varying either the $^{13}$C or $^{1}$H rf intensity during the contact time to achieve maximum signal), the duration of the $^{1}$H 90° pulse should be optimised (∼5 μs for the probe used).
5. The linewidths and signal-to-noise ratio from the set-up spectrum should be checked to ensure that resolution and sensitivity would be adequate for the sample of interest. Carbon-13 linewidths should be <10 Hz on mobile samples such as adamantane; larger linewidths imply poor shimming or some other experimental deficiency which should be corrected.
6. The sample should be packed into a rotor, which should be spun at a sufficiently high speed to avoid any spinning sidebands overlapping with peaks of interest (in this case ∼5 kHz was used).
7. Starting with the calibrated rf parameters, optimal values for the cross-polarisation contact time and recycle delay are determined in order to maximize sensitivity. In this case, we are quantifying the BHC signal and so these times were optimised for a pure BHC sample (5 s recycle delay and 5 ms contact time). The relatively short delay is useful, since it results in some discrimination against the dominant lactose signals, which have significantly longer relaxation times.

8. The NMR signal is then recorded with a sufficient acquisition time and number of transients to give both acceptable resolution and S/N in a reasonable total spectrometer time (2048 acquisitions taking ∼3 h in this case).

### 3.2. Processing data

The data are zero-filled to at least twice the acquisition length and mildly apodized to improve the spectral appearance, prior to Fourier transformation. Here we zero-filled to eight times the acquisition length, to give a spectrum with good digital resolution, and applied a 10 Hz Lorentzian line broadening.

The spectrum is "phased" to ensure that all the peaks appear as purely positive absorption signals, using a pair of intense peaks well-separated in the spectrum as guides (here the most intense lactose peak and methyl peak of the APIs). This is the only step of the processing and quantification that requires operator judgement.

The peaks of interest must be sitting on a flat baseline prior to quantification. Polynomial correction can be used to remove any baseline roll (provided there is sufficient clear baseline).

### 3.3. Measuring the peak area

Peaks areas can be obtained by integration or deconvolution (i.e. fitting to a model lineshape). Integration over a fixed range avoids systematic errors from fitting to a poor model function, but deconvolution is necessary if the peak of interest is overlapped, as in this case. Peaks at 147.3 ppm (BHC) and 34.2 ppm (magnesium stearate) were chosen for deconvolution, the latter supplying the necessary intensity reference.

As the lineshapes in solid-state NMR are rarely simple Lorentzians, the peaks are fitted to a mixed Lorentzian/Gaussian shape. The appropriate proportions for a given signal are determined from fitting the lineshape at high concentrations when the peaks are best defined. In our case, we found a 50% Gaussian/50% Lorentzian lineshape provided a good fit. The peaks of interest are iteratively fitted to this lineshape function to determine peak intensity.

### 3.4. Plot of composition versus peak area

A plot with molar composition (*x*-axis) of BHC versus measured ratio of peak areas for the chosen peaks of BHC and magnesium stearate (*y*-axis) is made. Such a plot is a pre-requisite for applying the protocol to a relevant sample of unknown BHC content. It is expected to be linear, so that only the slope is required accurately.

An error analysis should be carried out for the plot in order to understand the precision of the procedures. In our case we calculated the uncertainty arising from sample preparation, spectrometer conditions and processing the FID.

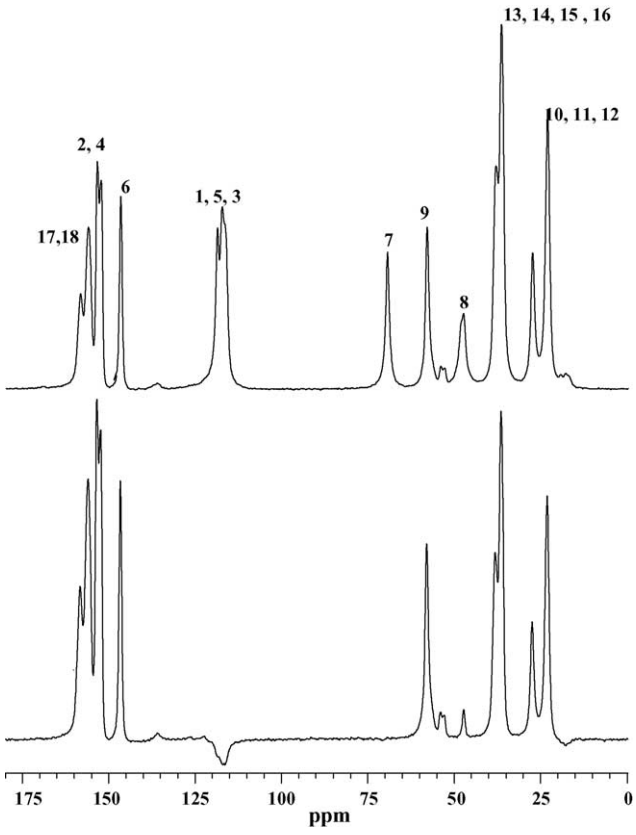


Fig. 2. Carbon-13 CPMAS spectra of BHC (form I). The lower spectrum was obtained with the dipolar dephasing ("non-quaternary suppression") experiment to suppress signals from CH and $CH_2$ sites.

## 4. Results and discussion

### 4.1. Carbon-13 spectra of BHC and TBS

Figs. 2 and 3 show the $^{13}C$ CPMAS spectra of microcrystalline BHC and TBS, respectively. The chemical shifts together with those obtained for solutions are listed in Tables 1 and 2. Assignments were assisted by use of $^{1}H$ solution-state spectra together with HSQC experiments and by using the dipolar dephasing experiment for the solid samples to suppress signals from CH and $CH_2$ sites. They were checked against semi-empirical predictions from 'Specinfo' [16].

Several features of the solid-state spectra are worthy of comment. For BHC, the splitting of the signal for C-2 and C-4, together with the lack of any splitting for C-6 and C-7 strongly suggests that the crystallographic asymmetric unit is one molecule, i.e. that the amide side-chains are non-equivalent. (Note that the crystal structure of BHC has not been reported.) The appearance of the resonance band for C-17 and C-18, together with the broadening observed for the C-6 signal, probably arises from second-order effects of the residual dipolar coupling to the $^{14}N$ nuclei [17]. The fact that the C-9 peak is relatively sharp suggests that the angle between the C-9 to nitrogen distance and the principal axis

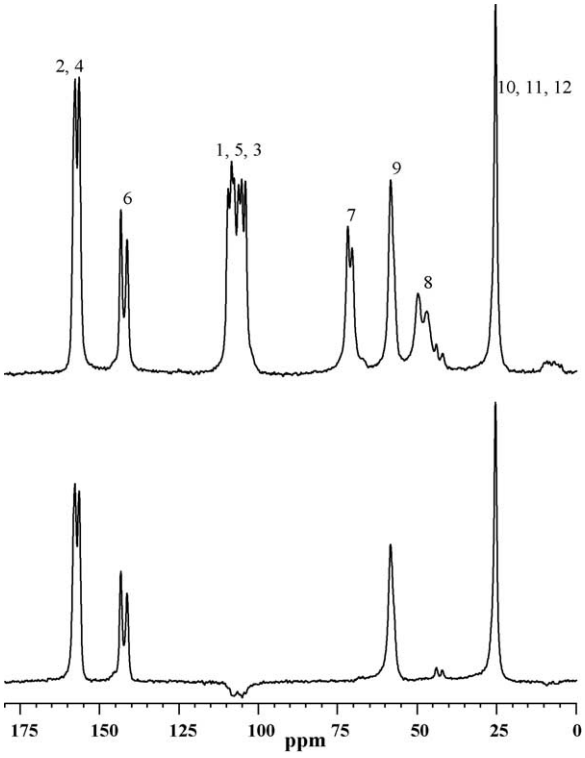


Fig. 3. Conventional (upper) and dipolar-dephased (lower) carbon-13 spectra of TBS (form B).

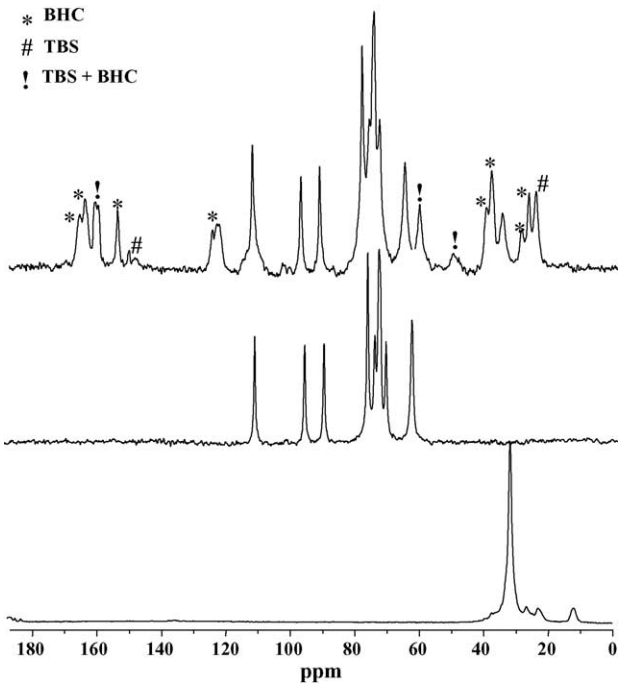


Fig. 4. Carbon-13 CPMAS spectrum of (top) the drug formulation (5% BHC tablets). The signals from the different drug components are marked by different symbols. Spectra of (middle) α-lactose monohydrate and (bottom) magnesium stearate are also shown.

of the electric field gradient at nitrogen is close to the magic angle. Perhaps, the most remarkable feature is the splitting for the methyl signals of the *t*-butyl group. Clearly, rotation about the C–N bond is strongly inhibited in the solid and one methyl is in a significantly different environment to the other two.

The solid-state spectrum of TBS (form B), shown in Fig. 3, is also of interest. The pair of lines seen for C-6 and also for C-7 shows unequivocally that the asymmetric unit comprises two molecules (as confirmed by the crystal structure [11]).

### 4.2. Spectra of the formulations

Fig. 4 shows the $^{13}C$ spectrum of tablets containing 5% BHC together with 5% TBS and 1% magnesium stearate, the remaining component being α-lactose monohydrate. The peaks of the drug constituents are indicated by different symbols with the resonances used for determining the concentration of BHC (namely that for C-6 of BHC at 147.3 ppm and that for magnesium stearate at 34.2 ppm) shown by arrows (see Fig. 5). The magnesium stearate peak is used as an internal reference to reduce the numerous systematic factors which would impact absolute quantification.

Fig. 5 gives the spectra (obtained under the standard conditions listed in the protocol above) for a range of BHC concentrations with the amount of TBS and magnesium stearate kept constant. Ratios between the areas (as obtained by deconvolution) of the chosen BHC and magnesium stearate peaks

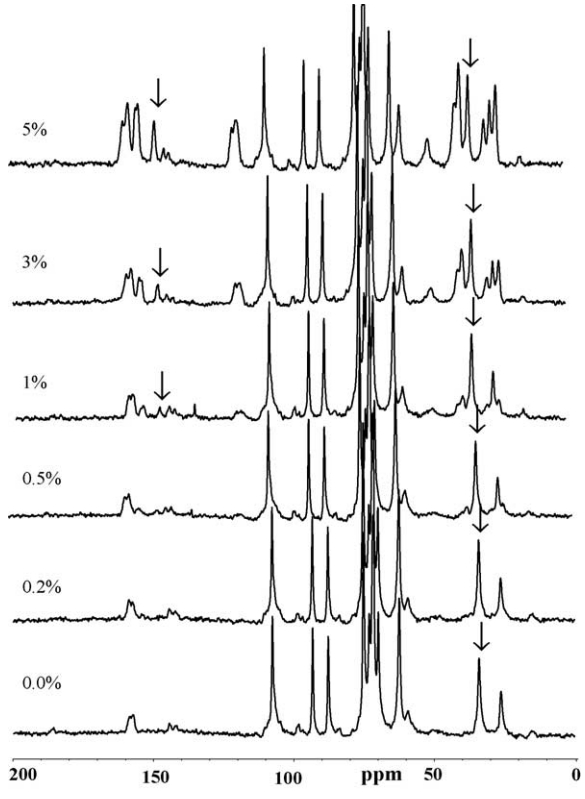


Fig. 5. Spectra of BHC tablets with various compositions. The percentages of BHC are given at the left-hand side of the figure. The peaks used for quantitation measurements are indicated by arrows.

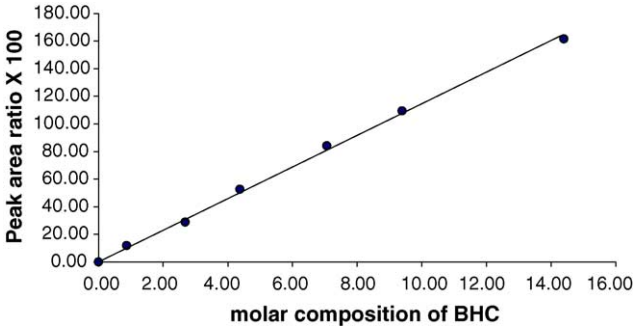


Fig. 6. Quantification calibration plot for BHC. The ordinate is the ratio (from deconvoluted peak areas), multiplied by 100, of the specified BHC and magnesium stearate signals. The concentrations are presented as mole%.

were used to establish the calibration plot of Fig. 6. The S/N of the selected BHC peak (defined as the rms deviation) for the 1% concentration was 4.2 and repetition (i.e. from spectra of separately prepared samples, see Fig. 7) gives values of 5.2 and 4.6. This shows the reproducibility that is achievable. Repeat measurements under different conditions (see below) provide evidence that 1% represents the LOQ under the conditions employed. Naturally this may be exceeded if a higher-field spectrometer or a significantly longer accumulation time is used. However, it is still possible to observe a peak at 147.3 ppm (with a S/N of ca. 2–3, see Fig. 5) for a 0.5% concentration, so this can be regarded as the LOD for these conditions. These values are, as far as we can determine, consistent with the definitions of LOD and LOQ in the literature [13,14].

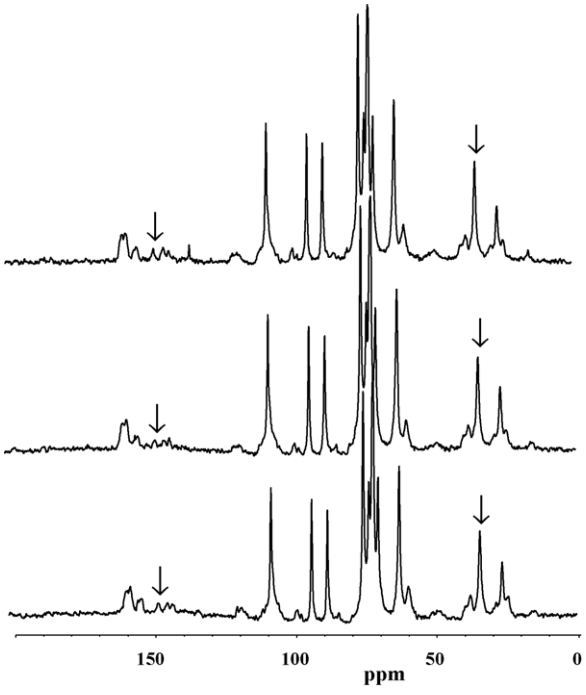


Fig. 7. Spectra showing the reproducibility in sample preparation for the 1% BHC case (see the text). The relevant peak area ratios are (top to bottom) 0.138, 0.142 and 0.142.

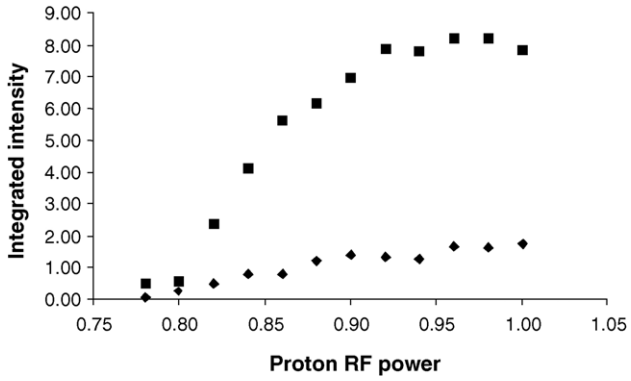


Fig. 8. Plot to show the effect of departure from the H–H matching condition on quantification. The lower curve is for the chosen BHC peak whereas the upper curve is for the reference magnesium stearate peak. The vertical axis is integrated intensity in arbitrary units. The horizontal axis represents the proton rf power (uncalibrated) relative to that required for the Hartmann–Hahn condition.

### 4.3. Sources of error on intensity measurement

Clearly, many factors which influence absolute intensities (such as variable sample volumes, spectrometer performance and $B_1$ inhomogeneity over the sample) will be compensated for by the use of relative quantification (e.g. with a magnesium stearate peak as an internal intensity reference, as in the present case), and so will only affect results to second order. Similarly, whilst the MAS rate will certainly influence the relative intensities of the chosen BHC and marker peaks, since their shielding anisotropies will differ, and hence the spinning sideband intensities will be differentially affected, use of a fixed spin rate will ensure that end results are not significantly influenced. The proton decoupler power will act analogously. To a considerable extent, any error in setting the Hartmann–Hahn condition will also be of low significance, as illustrated in Fig. 8, because of compensation arising from the use of an internal reference peak.

The limiting factor for quantification using $^{13}C$ at natural abundance is ultimately the noise level, which will alter the spectra, and hence integrals, in the region of measurement. We have evaluated this factor by repeated experiments for a single sample of 1% concentration, both in successive time periods (six measurements) and at random later intervals (seven measurements). The results for the mean of the BHC S/N plus/minus one standard deviation are $4.16 \pm 0.12$ and $4.41 \pm 0.27$ for these experiments, respectively. The uncertainty from the spectral measuring procedures alone is also calculated by processing a single FID several times and calculating the peak areas and mean, etc. The resulting percentage uncertainty produces error bars in the abscissa of the calibration curve (Fig. 6) for this effect, which are insignificant (with a standard deviation of 0.002–0.003, i.e. smaller than the size of the points as plotted).

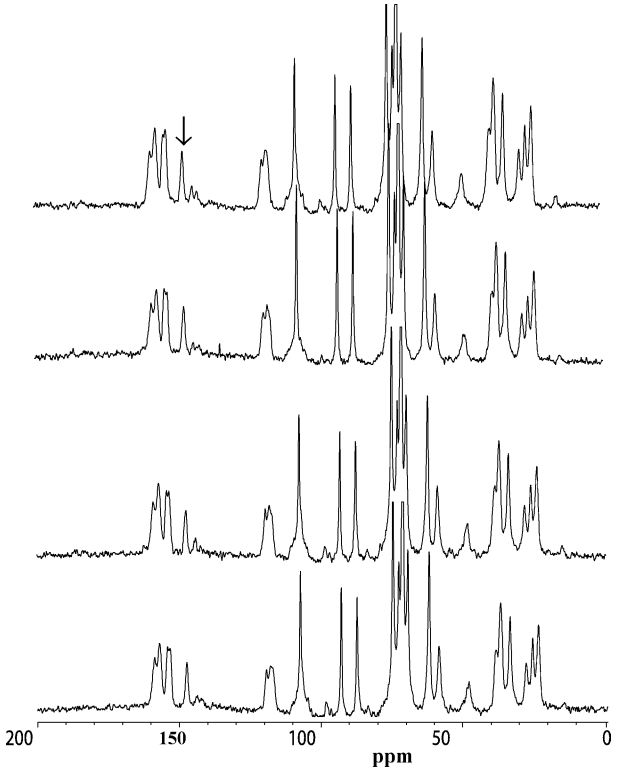


Fig. 9. Spectra of the 5% BHC composition obtained from samples in (top to bottom) tablet, physical mixture, mildly crushed tablet and finely ground tablet forms. The relevant peak intensity ratios are 0.546, 0.582, 0.560 and 0.581, respectively.

### *4.4. Errors dependent on sample preparation*

Errors in the ordinates of the points on the calibration graph will arise from inaccuracies in the preparation of the samples, but these will be largely obviated if enough points are used in the plot. A more serious practical problem would be if the spectra were significantly dependent on the nature of the sample preparation [18]. To judge whether grinding or compaction affects quantification, we have made measurements (see Fig. 9) on samples at the 5% concentration ratio obtained using (a) whole tablets produced as described in Section 2, (b) a simple physical mixture of the ingredients, (c) whole tablets mildly crushed and (d) whole tablets finely ground. The spectra are indistinguishable and the variations in the measured intensity (area) ratios of the two peaks (0.546, 0.582, 0.560 and 0.581, respectively) are within the expected experimental errors. Clearly, the measurements are not sensitive to the mode of sample preparation.

Whilst in the present sample we have chosen to use one of the common excipients to provide an internal reference standard, in many cases such a component might be expected to vary in intensity in different samples, so a known mass percentage of an additive would be recommended for this purpose.

## 5. Conclusions

Carbon-13 CPMAS spectra of BHC and TBS have been assigned and the crystallographic asymmetric units determined. A calibration plot for quantification of BHC in a formulated system has been produced, along with a protocol, which addresses the issues which can affect such measurements of quantification in solid-state NMR. The limits of detection and quantification of BHC under the given probe and acquisition conditions are 0.5 and 1%, respectively. Reproducibility in sample preparation and in quantification is good. There is no significant effect from tabulation or grinding in this particular case.

## Acknowledgements

The authors gratefully thank AstraZeneca R&D, Lund, Sweden, for the financial support for this project. We are also grateful to Dr. David C. Apperley and Dr. Walter Cook for useful discussions and also for assistance with the NMR and with the tablet manufacture, respectively. One of us (RKH) thanks the Leverhulme Trust for an Emeritus Fellowship.

## References

[1] T.L. Threlfall, Analyst 120 (1995) 2435–2460.
[2] S.R. Vippagunta, H.G. Brittain, D.J.W. Grant, Adv. Drug Deliv. Rev. 48 (2001) 3–26.
[3] G.A. Stephenson, R.A. Forbes, S.M. Reutzel-Edens, Adv. Drug Deliv. Rev. 48 (2001) 67–90.
[4] C.G. Campbell, L.G. Galya, A.J. Beeler, A.D. English, J. Magn. Reson. A 112 (1995) 225–228.
[5] J.Z. Hu, X. Wu, N. Yang, L. Li, C. Ye, K. Qin, Solid State NMR 6 (1996) 187–196.
[6] R.K. Harris, Analyst 110 (1985) 649–655.
[7] B. van Lagen, Fresenius Environ. Bull. 12 (2003) 1211–1217.
[8] R. Suryanarayanan, T.S. Wiedmann, Pharm. Res. 7 (1990) 184–187.
[9] Internal AstraZeneca Report.
[10] D. Hickel, A. Carpy, M. Laguerre, J.M. Leger, Acta Crystallogr. B38 (1982) 632–635.
[11] ICH-Q2B, Guideline for Industry. Validation of Analytical Procedures: Methodology. U.S. Department of Health & Human Services, 1996, http://www.fda.gov/cber/guidelines.htm.
[12] I. Taverniers, M. De Loose, E. Van Bockstaele, Trends Anal. Chem. 23 (2004) 535–552.
[13] J.C. Miller, J.N. Miller, Statistics for Analytical Chemistry, Ellis Harwood, London, 1993.
[14] ASTM, E685-93.
[15] S.J. Opella, M.H. Frey, J. Am. Chem. Soc. 101 (1979) 5854–5856.
[16] M.G. Weller, Recent Adv. Chem. Ref. 100 (1992) 197–208.
[17] R.K. Harris, A.C. Olivieri, Prog. NMR Spectrosc. 24 (1992) 435–456.
[18] K.R. Morris, U.L. Griesser, C.L. Eckhardt, J.G. Stowell, Adv. Drug Del. Rev. 48 (2001) 91–114.